

Anomalous Dome-like Superconductivity in $\text{RE}_2(\text{Cu}_{1-x}\text{Ni}_x)_5\text{As}_3\text{O}_2$ (RE=La, Pr, Nd)

Xu Chen,^{1,2,7} Jiangang Guo,^{1,7,8,*} Chunsheng Gong,¹ Erjian Cheng,³ Congcong Le,^{4,1}
Ning Liu,^{1,2} Tianping Ying,³ Qinghua Zhang,¹ Jiangping Hu,^{1,4,6} Shiyun Li,^{3,5} and
Xiaolong Chen^{1,2,6,*}

¹Beijing National Laboratory for Condensed Matter Physics, Institute of Physics, Chinese Academy of Sciences, P. O. Box 603, Beijing 100190, China

²University of Chinese Academy of Sciences, Beijing 100049, China

³State Key Laboratory of Surface Physics, Department of Physics, and Laboratory of Advanced Materials, Fudan University, Shanghai 200433, China

⁴Kavli Institute of Theoretical Sciences, University of Chinese Academy of Sciences, Beijing 100190, China

⁵Collaborative Innovation Center of Advanced Microstructures, Nanjing 210093, China

⁶Songshan Lake Materials Laboratory, Dongguan, Guangdong 523808, China

⁷These authors contributed equally

⁸Lead Contact

*Correspondence: jgguo@iphy.ac.cn (J.G.), chenx29@iphy.ac.cn (X.C.)

SUMMARY

Significant manifestation of interplay of superconductivity and charge density wave, spin density wave or magnetism is dome-like variation in superconducting critical temperature (T_c) for cuprate, iron-based and heavy Fermion superconductors. Overall behavior is that the ordered temperature is gradually suppressed and the T_c is enhanced under external control parameters. Many phenomena like pseudogap, quantum critical point and strange metal emerge in the different doping range. Exploring dome-shaped T_c in new superconductors is of importance to detect emergent effects. Here, we report that the observation of superconductivity in new layered Cu-based compound $\text{RE}_2\text{Cu}_5\text{As}_3\text{O}_2$ (RE=La, Pr, Nd), in which the T_c exhibits dome-like variation with maximum T_c of 2.5 K, 1.2 K and 1.0 K as substituting Cu by large amount of Ni ions. The transitions of T^* in former two compounds can be suppressed by either Ni doping or rare earth replacement. Simultaneously, the structural parameters like As-As bond length and c/a ratio exhibit unusual variations as Ni-doping level goes through the optimal value. The robustness of superconductivity, up to 60% of Ni doping, reveals the unexpected impurity effect on inducing and enhancing superconductivity in this novel layered materials.

INTRODUCTION

Cuprate superconductors are a class of layered compounds that belong to the regime of strongly-correlated electron system and their superconducting energy gaps are thought to be *d*-wave type (Wollman et al., 1993; Tsuei and Kirtley, 2000). Both magnetic and non-magnetic impurities in the Cu site will seriously suppress superconductivity (SC) (Xiao et al., 1990). Dome-like T_c often shows up when the carrier concentration increases from 5% to 25% by doping in non-CuO₂ layers (spacer layers) (Lee et al., 2006). For iron-based superconductors, carriers change by doping in non-SC layers may have a similar effect on T_c but the effect of impurities on the Fe site is totally different, which is regard as a signature of different superconducting gap symmetry details, S⁻ (Mazin, 2010; Mazin et al., 2008) or S⁺⁺ (Kuroki et al., 2008; Onari and Kontani, 2009). For example, partial substitution of O by F in LaFeAsO (Kamihara et al., 2008) or Ba by K in BaFe₂As₂ (Rotter et al., 2008) can lead to the dome-like T_c . Surprisingly, similar dome-shaped T_c also can be achieved by substituting Fe²⁺ by Co²⁺ or Ni²⁺ ions with more 3*d* electrons (Sefat et al., 2008; Canfield et al., 2009; Ni et al., 2010; Li et al., 2009). One explanation is that the doping is justified by the rigid-band model to some extent, where the doped electrons are in itinerant states, only shifting the Fermi level to the higher density of states (Ideta et al., 2013; Ideta et al., 2011). At the same time, the correlation strength of electrons and spin fluctuations might be drastically modified (Nakajima et al., 2014; Dai et al., 2012). As far as we know, such dome-like T_c induced by Ni²⁺ has not been known in other systems.

In this work, we report three novel layered superconductors, RE₂Cu₅As₃O₂ (RE=La, Pr, Nd), where Cu is coordinated by As in a new kind of [Cu₅As₃]²⁻ block. La₂Cu₅As₃O₂ (La2532) shows superconducting transition at $T_c = 0.63$ K while the latter Pr2532 and Nd2532 are non-superconducting phases. Strikingly, dome-like T_c emerges in RE₂(Cu_{1-x}Ni_x)₅As₃O₂ upon a wide range of Ni doping (0<*x*<0.6). These series of compounds exhibit different superconducting evolutions from both cuprate and iron-based superconductors. Our results highlight the role of Ni doping coupled with structural anomaly in inducing SC with Landau-Fermi liquid behavior.

RESULTS

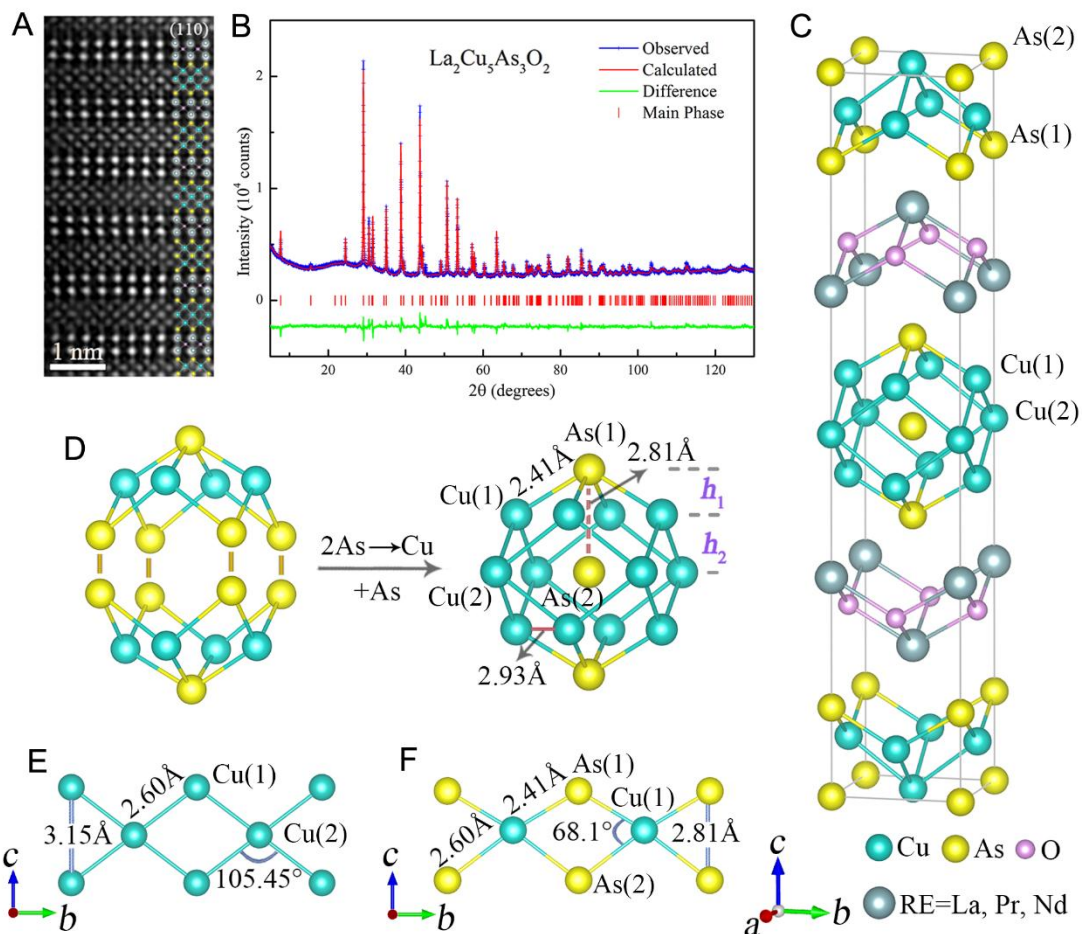


Figure 1. Structural determination, crystal structure and bonding details of $\text{RE}_2\text{Cu}_5\text{As}_3\text{O}_2$.

(A) HADDF image of (110) plane of $\text{La}_2\text{Cu}_5\text{As}_3\text{O}_2$.

(B) Rietveld refinement of PXRD of La2532 collected at 300 K.

(C) Crystal structure of $\text{RE}_2\text{Cu}_5\text{As}_3\text{O}_2$ (RE=La, Pr, Nd).

(D) $[\text{Cu}_5\text{As}_3]^{2-}$ unit is a combination of two Cu_2As_2 layers with replacing two As atoms by Cu atom. One more As atom is encapsulated in the center.

(E-F) Structural details of Cu network and Cu-As fragment.

Fig. 1A shows the HADDF image of (110) plane of La2532, in which two different slabs stack along the c -axis, indicating a typical layered structure. The collected powder X-ray diffraction (PXRD) pattern of La2532 can be indexed by a body-center tetragonal cell with space group $I4/mmm$ (No. 139). The refined lattice constants are

$a=b=4.1386(1)$ Å and $c=22.8678(6)$ Å. We construct the initial model by setting La1 4e (0.5, 0.5, z1), O1 4d (0.5, 0, 0.25), Cu(1) 8g (0.5, 0, z2), Cu(2) 2b (0, 0, 0.5), As(1) 4e (0, 0, z3) and As(2) 2a (0, 0, 0) as per $I4/mmm$. The Rietveld refinement successfully converges to $R_p=2.95\%$, $R_{wp}=4.26\%$ and $\chi^2=3.87$, and the refined patterns are shown in Fig. 1B. Pr2532 and Nd2532 are found to be isostructural to La2532 with lattice parameters $a=4.0802(1)$ Å and $c=22.9144(5)$ Å, $a=4.0561(1)$ Å and $c=23.0082(6)$ Å, respectively. The crystallographic parameters of RE2532 (RE=La, Pr, Nd) are summarized in Table S1 of SM.

The crystal structure of RE2532 is drawn in Fig. 1C, one can see that the $[\text{Cu}_5\text{As}_3]^{2-}$ blocks and the fluorite RE_2O_2 layers stack along c -axis, which agrees with the atomic distributions in HADDF image and stoichiometry of EDS analysis (Fig. S1). Figure 1D is structural detail of the $[\text{Cu}_5\text{As}_3]^{2-}$ block, which can be viewed as replacing neighbor As^{3-} anions of two Cu_2As_2 layers by one Cu atom. The bond lengths of Cu(1)-As(1) and Cu(1)-Cu(1) are 2.41 Å and 2.93 Å, respectively, close to the values in BaCu_2As_2 (Saparov and Sefat, 2012). It is noted that the bond length of As(1)-As(2), 2.81 Å, locates at the bonding regime of As-As covalent bond, 2.7~2.9 Å (Yakita et al., 2014). The $[\text{Cu}_5\text{As}_3]^{2-}$ unit is analogous to $[\text{Cu}_6\text{Pn}_2]^{2-}$ in BaCu_6Pn_2 (Pn=As, P) (Dünner and Mewis, 1995), where the central As atom is replaced by one Cu(2) atom. In Fig. 1, E and F, we can see that metallic bond of Cu-Cu exists in Cu network along b -axis as indicated by bond length, 2.60 Å, of Cu(1)-Cu(2). In coordination environment of Cu(1), short Cu(1)-As(1) and Cu(1)-As(2) bond lengths, 2.41 Å and 2.60 Å, suggest the covalence nature in $[\text{Cu}_5\text{As}_3]^{2-}$ unit like those Fe-As bonds in $[\text{Fe}_2\text{As}_2]^{2-}$ layers of iron-based superconductors (Huang et al., 2008).

The electrical resistivity of $\text{RE}_2\text{Cu}_5\text{As}_3\text{O}_2$ from 300 K to 1.8 K is plotted in Fig. 2, A and B. All data exhibits metallic behaviors, which can be fitted by $\rho \sim T^2$ at low temperature range, obeying the Fermi-liquid behavior, see the details in Fig. S2. There are resistivity kinks for La2532 and Pr2532 at $T^*=80$ K and 40 K, respectively. The external magnetic fields up to 9 T do not weaken this kink. However, for Nd2532, there is no any resistivity kink above 1.8 K. Measuring the resistivity at very low temperature reveals that La2532 is a superconductor with $T_c^{\text{onset}}=0.63$ K and

$T_c^{\text{zero}}=0.26$ K, as shown in the inset of Fig. 2A. The transition is suppressed by external magnetic field and finally disappears as $B>0.12$ T. The upper critical fields $\mu_0 H_{c2}(0)$, 0.15 T and 0.18 T, are estimated from the linear and Ginzburg-Landau (GL) fitting, respectively (Fig. S3). In contrast, the Pr2532 and Nd2532 are not superconductors above 0.25 K. This difference is possibly similar to the effect of suppressed SC in Pr-based cuprates (Chen et al., 1995; Chen et al., 1992).

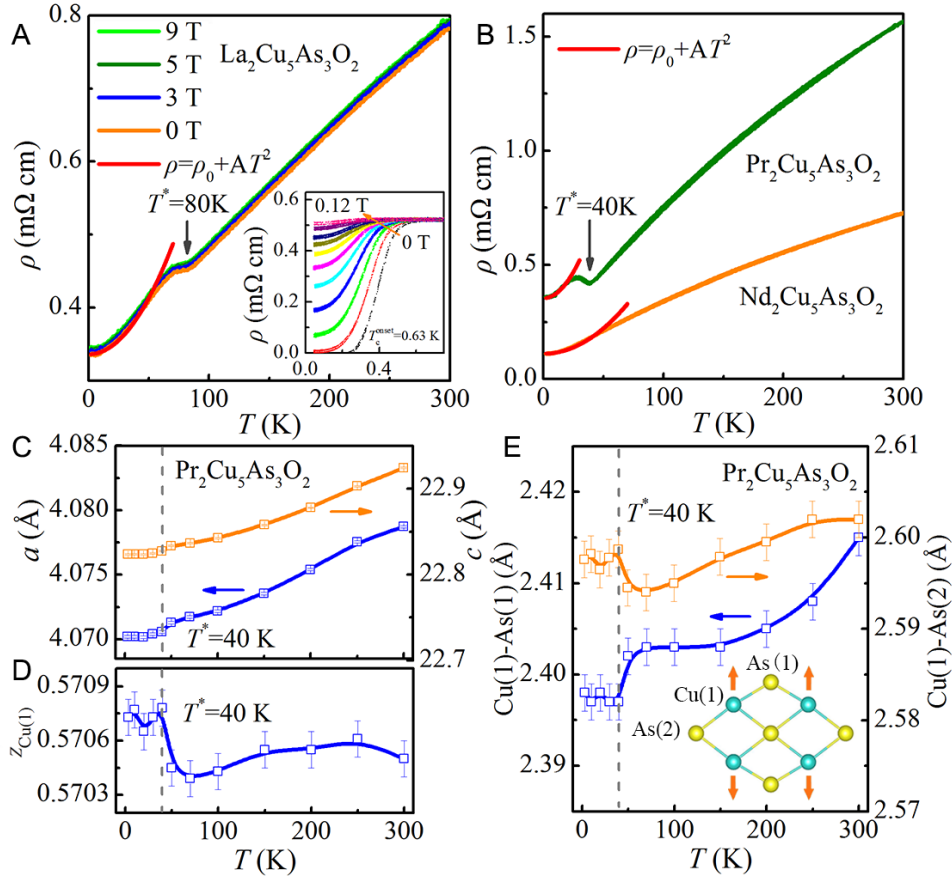


Figure 2. Transport properties and crystal structure at various temperatures.

(A-B) Normal-state electrical resistivity of $\text{RE}_2\text{Cu}_5\text{As}_3\text{O}_2$ as a function of temperature from 1.8 K-300 K. The data below T^* can be fitted by Fermi-liquid equation. The inset is the electrical resistivity of $\text{La}_2\text{Cu}_5\text{As}_3\text{O}_2$ around T_c under external magnetic field.

(C-D) Temperature-dependent a , c and $z_{\text{Cu}(1)}$ of Pr2532.

(E) The Cu(1)-As(1) and Cu(1)-As(2) bond lengths versus temperature. Inset shows schematic variation of Cu(1) below T^* .

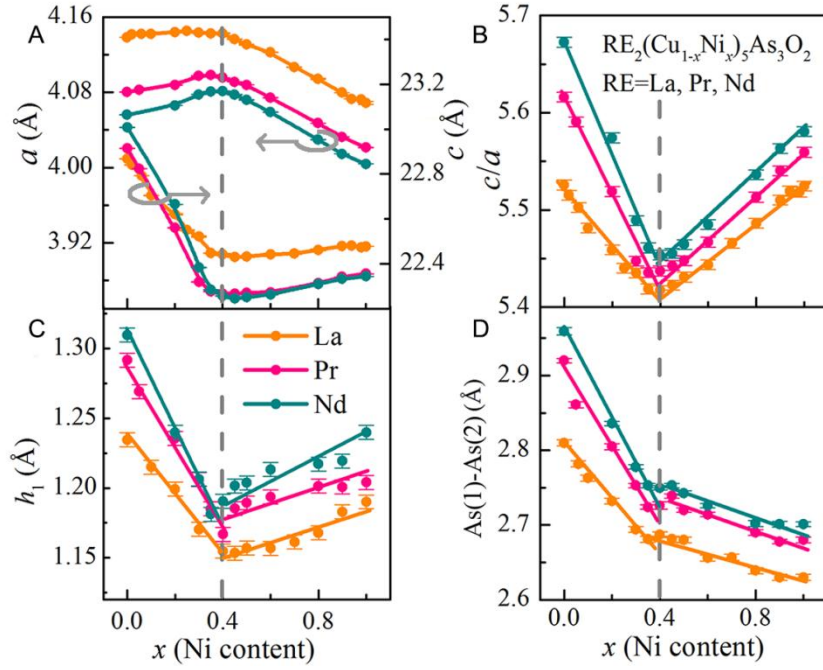


Figure 3. Selected crystallographic parameters of $\text{RE}_2(\text{Cu}_{1-x}\text{Ni}_x)_5\text{As}_3\text{O}_2$ as a function of Ni content.

(A) a and c . (B) c/a ratio. (C) As height (h_1). (D) As(1)-As(2) bond length.

The magnetic susceptibility (χ) and specific heat (C_p) at low temperatures were measured and plotted in Fig. S4. The fitting of $\chi(T)$ gives the effective magnetic moment $\mu_{\text{eff}} = 0.16 \mu_B$ and $\theta = -148(1)$ K, implying an anti-ferromagnetism (AFM) interaction of Cu ions. Furthermore, the fitting of C_p yields that Debye temperature Θ_D is 169(2) K and Sommerfeld coefficient $\gamma_0 = 5.01 \text{ mJ} \cdot \text{mol}^{-1} \cdot \text{K}^{-2}$ for La2532. We rule out the possibility of charge-density-wave transition by measuring the TEM of La2532 at low temperature, see Fig. S5. Meanwhile, the Rietveld refinement of temperature-dependent PXRD patterns of Pr2532 reveals that the a -axis and c -axis shrink on cooling, but both values show slightly discontinuity at 40 K, implying a structural distortion, see Fig. 2C and Fig. S6. In Fig. 2D, it is found that the $z_{\text{Cu}(1)}$ anomaly increases below 40 K. It leads to abrupt contraction of Cu(1)-As(1) bond and elongation of Cu(1)-As(2) bond, which enhances the structural anisotropy of $[\text{Cu}_5\text{As}_3]^{2-}$, as shown in Fig. 2E. Such change could induce charge redistribution and small resistivity jump. It is similar to the structural change and resistivity jump in

KNi₂S₂ (Neilson et al., 2013).

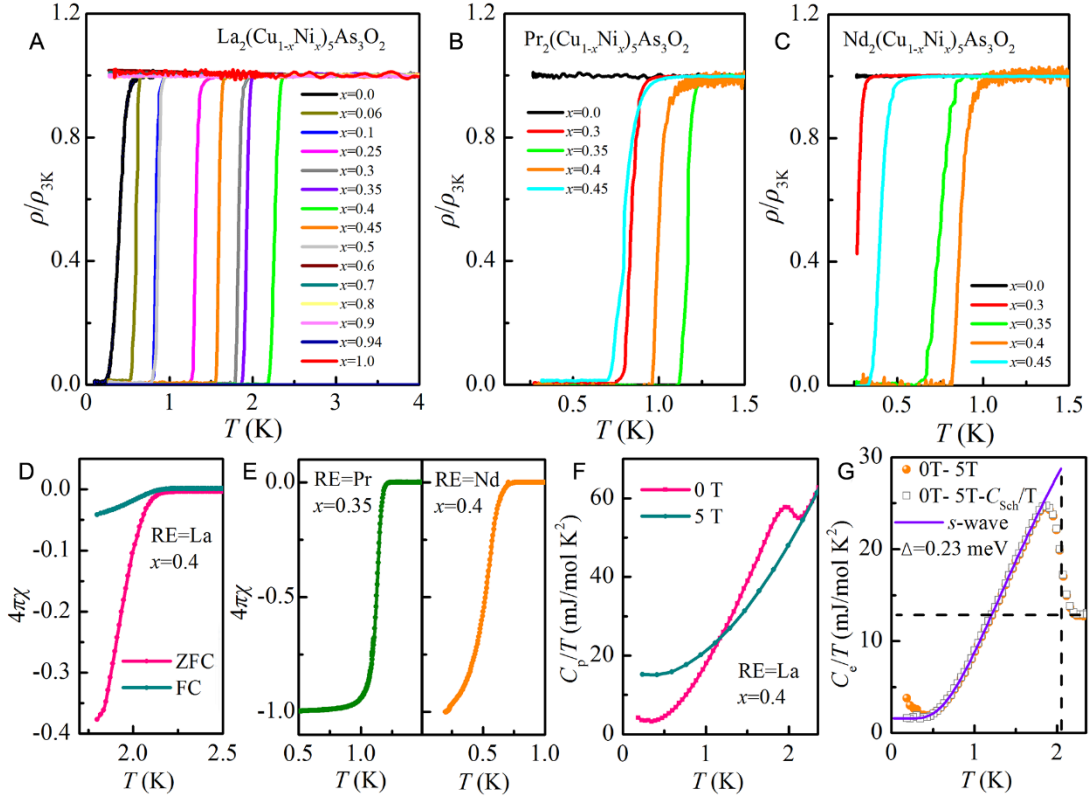


Figure 4. Physical properties of RE₂(Cu_{1-x}Ni_x)₅As₃O₂ (RE= La, Pr, Nd).

(A-C) Superconducting transition of RE₂(Cu_{1-x}Ni_x)₅As₃O₂. It can be found that the T_c firstly increases to maximum and then decreases to zero as increasing x .

(D-E) Superconducting volume fraction for $x \sim 0.4$ and RE=La, Pr, Nd samples at 10 Oe.

(F) C_p/T of La₂(Cu_{0.6}Ni_{0.4})₅As₃O₂ as a function of temperature under 0 T and 5 T.

(G) C_e/T and the fitting curves of La₂(Cu_{0.6}Ni_{0.4})₅As₃O₂ against temperature.

We prepared a series of RE₂(Cu_{1-x}Ni_x)₅As₃O₂ ($x=0-1.0$) samples so as to further explore the evolution SC against Ni substitution. The PXRD confirms RE₂(Cu_{1-x}Ni_x)₅As₃O₂ is a continuous solid solution, judging from the linear decrease in volume of unit cell (Fig. S7). The results of Rietveld refinement for all patterns are listed in Table S1. Selected crystallographic parameters are plotted in Fig. 3. One can see that the c -axis decreases drastically as $x < 0.4$, but the a -axis almost keeps constant, however, this variation is reversed as $x > 0.4$, see Fig. 3A. This anomalous feature makes the c/a ratio initially decreases as $x < 0.4$ while it starts to increase as

$x > 0.4$, where the minimum shows up at $x = 0.4$ shown in Fig. 3B. To our best knowledge, the structural changes of a , c and 'V' shape of c/a ratio are rare in layer superconductors. In Fig. 3C, the As height (h_1) firstly decreases as $x < 0.4$ and then increases, where the crossover perfectly matches the structural anomaly $x = 0.4$. The h_2 only linearly decreases upon Ni doping. The distinct variations of h_1 and h_2 induce a crossover of shrunk As(1)-As(2) bond length at $x = 0.4$, see Fig. 3D. On the other hand, since the Ni-doping changes the coordination environment of Cu(1), and the Cu(2)-As(2) bond length ($\sqrt{2} \cdot a/2$) almost keeps a constant, we speculate that the Ni firstly occupies the Cu(1) site as $x < 0.4$, shortening the h_1 and c -axis.

The electrical resistivity of $\text{RE}_2(\text{Cu}_{1-x}\text{Ni}_x)_5\text{As}_3\text{O}_2$ at low temperature are shown in Fig. 4A-C. For $\text{La}_2(\text{Cu}_{1-x}\text{Ni}_x)_5\text{As}_3\text{O}_2$, the T_c^{onset} monotonously increases to the maximal 2.5 K as $x = 0.4$. It is surprised that SC can be induced in the non-superconducting Pr2532 and Nd2532 by Ni doping, in which the T_c^{onset} also increases to the highest value 1.2 K and 1.0 K as $x \sim 0.4$, respectively. Once x is above 0.4, the T_c^{onset} gradually decreases and finally vanishes up to 0.6. The external magnetic fields smoothly suppress the SC off, and the $\mu_0 H'_{c2}(0)$ for three optimal-doped samples are 3.8 T (3.0 T), 0.69 T (0.52 T) and 0.54 T (0.37 T) estimated from the linear (GL) fitting, respectively (Fig. S8). In Fig. 4, D and E, the magnetization of three optimal-doped samples exhibit large superconducting volume fractions, indicating a bulk SC. Furthermore, the bulk SC of $\text{La}_2(\text{Cu}_{0.6}\text{Ni}_{0.4})_5\text{As}_3\text{O}_2$ is confirmed by a large superconducting jump in the specific heat (C_p). The magnetic field up to 5 T totally suppresses the SC, as seen from Fig. 4F. We fit the $C_p(5\text{T})$ data using the equation $C_p/T = \gamma + \beta T^2$, and obtain the $\gamma = 12.62 \text{ mJ} \cdot \text{mol}^{-1} \cdot \text{K}^{-2}$, $\beta = 9.89 \text{ mJ} \cdot \text{mol}^{-1} \cdot \text{K}^{-4}$ and $\Theta_D = 133(2) \text{ K}$. Extrapolating the data to 0 K finds a residual γ_n is $1.58 \text{ mJ} \cdot \text{mol}^{-1} \cdot \text{K}^{-2}$, indicating that the non-superconducting phase is $\sim 12.5\%$ due to impurity. Thus we obtain the superconducting γ_s is $11.04 \text{ mJ} \cdot \text{mol}^{-1} \cdot \text{K}^{-2}$, which results in the dimensionless jump of $C_e/\gamma_s T_c$ is 1.42, see Fig. 4G. This value is consistent with the BCS weak-coupling limit (1.43), but smaller than that of the optimal K-doped BaFe_2As_2 (2.5) (Popovich et al., 2010). We subtract the upturn of C_e/T at very low temperature due to Schottky anomaly using the treatment in Ref.

(Mu et al., 2007) and obtain the flatten C_e/T . As the BCS theory, $C_e/T \propto \exp[-\frac{\Delta(0)}{k_B T}]$, the data are fitted, yielding superconducting gap $\Delta(0)=0.23$ meV= $2.65k_B$ K. Knowing the $\Delta(0)$, a $2\Delta(0)/k_B T_c$ is 2.58, which is smaller than the weak-coupling limit (3.52) within the BCS framework. The estimation of the Schottky anomaly and semi-logarithmic of C_e/T are shown in Fig. S9. Note that subtracting of Schottky anomaly possibly undermines the rationality of s-wave SC.

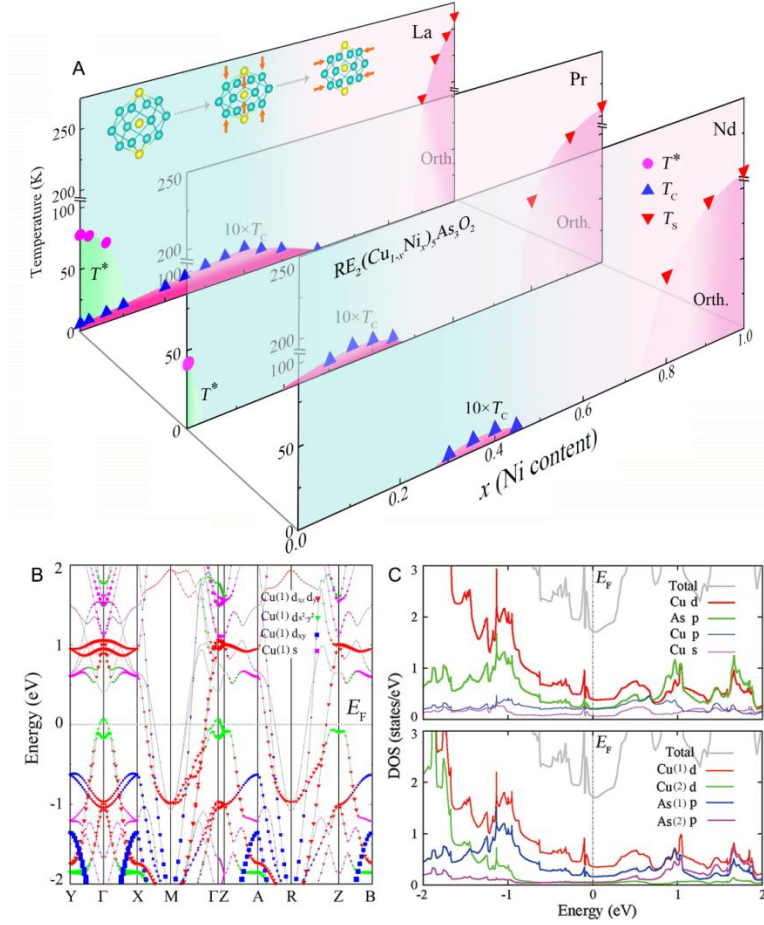


Figure 5. Phase diagram of $RE_2(Cu_{1-x}Ni_x)_5As_3O_2$ and electronic structure of $La_2Cu_5As_3O_2$.

(A) Phase diagram of $RE_2(Cu_{1-x}Ni_x)_5As_3O_2$. It can be seen that the T^* is suppressed and dome-like T_c shows up. The inset shows that the structure of $[Cu_5As_3]^{2-}$ unit changes upon Ni doping.

(B) Cu(1) orbital-weighted band structures of $La_2Cu_5As_3O_2$.

(C) Upper panel: the projected density of states of Cu d , p , s , and As p orbitals at the ranges of -2 eV to 2 eV. Lower panel: the projected density of states of different Cu

and As site, showing the Cu(1) d and As(1) p orbitals dominate at the Fermi level.

The electrical resistivity of $\text{RE}_2(\text{Cu}_{1-x}\text{Ni}_x)_5\text{As}_3\text{O}_2$ from 1.8 K-300 K shows that the T^* is rapidly suppressed upon slight Ni-doping ($x < 0.1$) as shown in Fig. S10. In end-member $\text{La}_2\text{Ni}_5\text{As}_3\text{O}_2$, $\text{Pr}_2\text{Ni}_5\text{As}_3\text{O}_2$ and $\text{Nd}_2\text{Ni}_5\text{As}_3\text{O}_2$, another resistivity anomaly associated with structural transition shows up, where the T_s are 260 K, 210 K and 190 K, respectively. Indexing temperature-dependent PXRD patterns of $\text{La}_2(\text{Cu}_{0.02}\text{Ni}_{0.98})_5\text{As}_3\text{O}_2$ found that the (200) and (215) peaks split into (020)/(200) and (125)/(215) peaks below T_s , indicating a symmetry breaking from tetragonal (C_4) to orthorhombic phase (C_2 , I mmm, No. 71) (Fig. S11). We can map out the electronic phase diagram of $\text{RE}_2(\text{Cu}_{1-x}\text{Ni}_x)_5\text{As}_3\text{O}_2$, see Fig. 5A. Most interesting thing is that dome-like T_c can be observed, where the superconducting phases emerge at $0 < x < 0.6$, $0.2 < x < 0.45$ and $0.3 < x < 0.45$ for Ni-doped La2532, Pr2532 and Nd2532, respectively. The enhancement of SC upon Ni is rather rare, which is only observed in iron-based superconductors (Sefat et al., 2008; Ni et al., 2010). Furthermore, in terms of crystal structure, this enhancement is related to squeezing the $[\text{Cu}_5\text{As}_3]^{2-}$ along c -axis as $x < 0.4$, and the suppression of T_c corresponds to a contraction of $[\text{Cu}_5\text{As}_3]^{2-}$ along a -axis, shown as inset of Fig. 5A. The phase diagram is similar to those of cuprates and iron-based superconductors to large extent, which features the competition of structural distortion and SC.

DISCUSSION

We calculated the electronic structure in the paramagnetic state from DFT calculations. The band structures of La2532 are shown in Fig. 5B, where a small hole-pocket and three large electron-pockets show up at the Γ and M point, respectively. Around E_F , the bands along the Γ -X and Γ -Y directions have large dispersion while the bands along Γ -Z are almost flat, indicating that the Fermi surfaces are quasi-two-dimensional. The hole-pocket is mainly composed of Cu(1) $d_{x^2-y^2}$ hybridizing with As(1) P_z , and the electron-pockets components are Cu(1) d_{xz}/d_{yz} , d_{xy} and As(1) $P_{x/y}$ (Fig. S12). It is noted that the Cu(1) d_{xz}/d_{yz} dominate the states at Fermi energy (E_F), different from that in cuprates superconductors (Uchida,

2015). In Fig. 5C, one clearly sees that the E_F is dominated by Cu(1) d and As(1) p states. There are higher $N(E_F)$ at -0.1 eV below E_F , therefore, doping Ni with one electron less can lower the E_F , which is theoretically reasonable to induce higher $N(E_F)$ and T_c . The total $N(E_F)$ is 1.75 states/eV f. u. and the estimated bare Sommerfeld coefficient is $2.06 \text{ mJ mol}^{-1} \text{ K}^{-2}$. According to the equation $\gamma_n = \gamma_b(1 + \lambda_{e-p})(1 + \lambda_{e-e})$, if we assume the electron-electron coupling $\lambda_{e-e} = 0$, one would can obtain an electron-phonon coupling $\lambda_{e-p} = 1.43$. The large λ_{e-p} exceeds the limit of BCS framework, implying that the electron-electron coupling cannot be ignored.

It is previously reported that the bonded anionic dimer can induce ferromagnetic critical point, SC and metal-insulator transition (**Jia et al., 2011; Guo et al., 2012; Radaelli et al., 2002**). Here, there are weak bonding states of As(1)-As(2) in $\text{RE}_2\text{Cu}_5\text{As}_3\text{O}_{12}$, and the E_F will be higher than the bonding orbital (σ), and locates the bottom of the anti-bonding orbital (σ^*) (**Hoffmann and Zheng, 1985; Hoffmann, 1988**). As $x < 0.4$, the doped holes would firstly enter into the As(1)-As(2) bond and lift the valence of As^{3-} . The strengthened bond between apical As(1)-central As(2) rapidly shortens the c -axis. At the same time, the E_F slowly drops to the energy between σ and σ^* orbital. As $x > 0.4$, the shrinking of As(1)-As(2) bond length and c -axis slows, and then the a -axis begin to quickly decreases. It means that some of excess holes are introduced into the lattice, which possibly suppresses the SC. The Hall measurement, shown in Fig. S13, shows positive Hall coefficients. It indicates that the dominated carriers are holes. Using the single-band model, we obtain the carrier concentration is $\sim 10^{22} \text{ cm}^{-3}$, which is slightly increased in 40% Ni-doped La2532.

Still, the static magnetic order associated with Cu ions is not observed in all measured samples above 1.8 K, and all the $\chi(T)$ curves can be fitted by Curie-Weiss equation, see Fig. S14. The $4f^0$ La2532 is an itinerant compound with AFM interaction ($\mu_{\text{eff}} = 0.16 \mu_B$ per Cu; $\theta = -148 \text{ K}$). For 40% and 100% Ni-doped La2532, the resultant μ_{eff} and θ are $0.56 \mu_B/\text{Cu}$, -256 K and $0.69 \mu_B/\text{Cu}$, -424 K , respectively. It means that the Ni-doped samples have larger μ_{eff} and stronger AFM interaction. However, these moments are still much smaller than the theoretical value ($1.73 \mu_B$) for Cu^{2+} ions with $S = 1/2$. It means that the magnetic interaction is not fully localized, and the

emergence of Cu-Cu metallic bonds in $[\text{Cu}_5\text{As}_3]^{2-}$ significantly increases the amount of itinerant electrons. The superconductivity here is likely to be itinerant picture (**Singh and Du, 2008; Dong et al., 2008**), which is similar to those of BaNi_2As_2 and LaNiAsO (**Subedi and Singh, 2008; Boeri et al., 2009**). In $\text{Pr}_2\text{532}$ and $\text{Nd}_2\text{532}$, the total μ_{eff} and θ are $4.42 \mu_{\text{B}}/\text{Pr}$ and -26.5 K , $4.62 \mu_{\text{B}}/\text{Nd}$ and -30.4 K , respectively. The μ_{eff} is larger than the values for the magnetic Pr^{3+} ($4f^2$, $3.58 \mu_{\text{B}}$) and Nd^{3+} ($4f^3$, $3.62 \mu_{\text{B}}$) in Ni-based superconductors (**Li et al., 2014**), indicating that the magnetic contribution of Cu ions is important. Since the carrier doping can suppress the moment of RE^{3+} (**Zhao et al., 2008**), we cannot summarize clear variation of magnetic moment of Cu ions in Ni-doped $\text{Pr}_2\text{532}$ and $\text{Nd}_2\text{532}$. High-precision experiments are called for to identify the Cu's magnetism.

The results provide a novel kind of Cu-based superconductor $\text{RE}_2\text{Cu}_5\text{As}_3\text{O}_2$ ($\text{RE}=\text{La}, \text{Pr}, \text{Nd}$), whose crystal structure, SC and ground states can be effectively tuned through rather wide range of Ni doping. The dome-like T_c in turn is induced by the dimerization of As-As bonds along c -axis and shrinking of a -axis. The robust SC against Ni, structural anomaly and enhanced AFM interaction provides new perspectives to understand the superconducting mechanism.

METHODS

All methods can be found in the accompanying Transparent Methods supplemental file.

SUPPLEMENTAL INFORMATION

Supplemental Information includes Transparent Methods, 14 figures, and 1 tables

ACKNOWLEDGMENTS

We acknowledge H. Hosono, H. Ding and Y. Zhang for valuable discussions and TEM measurement. This work was supported by the National Key Research and Development Program of China (No. 2017YFA0304700, 2016YFA0300600), the National Natural Science Foundation of China (No. 51772322, 51532010), and the Strategic Priority Research Program and Key Research Program of Frontier Sciences of the Chinese Academy of Sciences (No. QYZDJ-SSW-SLH013).

AUTHOR CONTRIBUTIONS

J. G and X. L. C. provided strategy and advice for the material exploration. X. C., J. G. and C. Gong performed the sample fabrication, measurements and fundamental data analysis. E. C., T. Y. and S. L. measured the low temperature properties. C. L., N. L. and J. H. carried out the theoretical calculation. Q. Z. measured the HAADF images. J. G. and X. L. C. wrote the manuscript based on discussion with all the authors.

DECLARATION OF INTERESTS

The authors declare no competing interests.

REFERENCES AND NOTES

Wollman, D.A., Vanharlingen, D.J., Lee, W.C., Ginsberg, D.M., and Leggett, A.J. (1993). Experimental determination of the superconducting pairing state in YBCO from the phase coherence of YBCO-Pb dc SQUIDs. *Phys. Rev. Lett.* *71*, 2134-2137.

Tsuei, C.C., and Kirtley, J.R. (2000). Pairing symmetry in cuprate superconductors. *Rev. Mod. Phys.* *72*, 969-1016.

Xiao, G., Cieplak, M.Z., Xiao, J.Q., and Chien, C.L. (1990). Magnetic pair-breaking effects: Moment formation and critical doping level in superconducting $\text{La}_{1.85}\text{Sr}_{0.15}\text{Cu}_{1-x}\text{A}_x\text{O}_4$ systems (A=Fe, Co, Ni, Zn, Ga, Al). *Phys. Rev. B* *42*, 8752.

Lee, P.A., Nagaosa, N., and Wen, X.G. (2006). Doping a Mott insulator: Physics of high-temperature superconductivity. *Rev. Mod. Phys.* *78*, 17-85.

Mazin, I.I. (2010). Superconductivity gets an iron boost. *Nature* *464*, 183.

Mazin, I.I., Singh, D.J., Johannes, M.D., and Du, M.H. (2008). Unconventional superconductivity with a sign reversal in the order parameter of $\text{LaFeAsO}_{1-x}\text{F}_x$. *Phys. Rev. Lett.* *101*, 057003.

Kuroki, K., Onari, S., Arita, R., Usui, H., Tanaka, Y., Kontani, H., and Aoki, H. (2008). Unconventional pairing originating from the disconnected Fermi surfaces of superconducting $\text{LaFeAsO}_{1-x}\text{F}_x$. *Phys. Rev. Lett.* *101*, 087004.

Onari, S., and Kontani, H. (2009). Violation of Anderson's theorem for the sign-reversing s-wave state of iron-pnictide superconductors. *Phys. Rev. Lett.* *103*, 177001.

Kamihara, Y., Watanabe, T., Hirano, M., and Hosono, H. (2008). Iron-based layered superconductor $\text{La}[\text{O}_{1-x}\text{F}_x]\text{FeAs}$ ($x=0.05-0.12$) with $T_c=26$ K. *J. Am. Chem. Soc.* *130*, 3296-3297

Rotter, M., Tegel, M., and Johrendt, D. (2008). Superconductivity at 38 K in the iron arsenide $(\text{Ba}_{1-x}\text{K}_x)\text{Fe}_2\text{As}_2$. *Phys. Rev. Lett.* *101*, 107006.

Sefat, A.S., Jin, R., McGuire, M.A., Sales, B.C., Singh, D.J., and Mandrus, D. (2008). Superconductivity at 22 K in Co-doped BaFe₂As₂ crystals. *Phys. Rev. Lett.* *101*, 117004.

Canfield, P.C., Bud'ko, S.L., Ni, N., Yan, J.Q., and Kracher, A. (2009). Decoupling of the superconducting and magnetic/structural phase transitions in electron-doped BaFe₂As₂. *Phys. Rev. B* *80*, 060501(R).

Ni, N., Thaler, A., Yan, J.Q., Kracher, A., Colombier, E., Bud'ko, S.L., Canfield, P.C., and Hannahs, S.T. (2010). Temperature versus doping phase diagrams for Ba(Fe_{1-x}TM_x)₂As₂ (TM=Ni, Cu, Cu/Co) single crystals. *Phys. Rev. B* *82*, 024519.

Li, L.J., Luo, Y.K., Wang, Q.B., Chen, H., Ren, Z., Tao, Q., Li, Y.K., Lin, X., He, M., Zhu, Z.W., Cao, G.H., and Xu, Z.A. (2009). Superconductivity induced by Ni doping in BaFe₂As₂ single crystals. *New J. Phys.* *11*, 025008.

Ideta, S., Yoshida, T., Nishi, I., Fujimori, A., Kotani, Y., Ono, K., Nakashima, Y., Yamaichi, S., Sasagawa, T., Nakajima, M., Kihou, K., Tomioka, Y., Lee, C.H., Iyo, A., Eisaki, H., Ito, T., Uchida, S., and Arita, R. (2013). Dependence of carrier doping on the impurity potential in transition-metal-substituted FeAs-based superconductors. *Phys. Rev. Lett.* *110*, 107007.

Ideta, S., Yoshida, T., Nishi, I., Fujimori, A., Kotani, Y., Ono, K., Nakashima, Y., Yamaichi, S., Sasagawa, T., Nakajima, M., Kihou, K., Tomioka, Y., Lee, C.H., Iyo, A., Eisaki, H., Ito, T., Uchida, S., and Arita, R. (2011). Fermi-surface evolution by transition-metal substitution in the iron-based superconductor LaFeAsO. *J. Phys. Soc. Jpn.* *80*, 123701.

Nakajima, M., Ishida, S., Tanaka, T., Kihou, K., Tomioka, Y., Saito, T., Lee, C.H., Fukazawa, H., Kohori, Y., Kakeshita, T., Iyo, A., Ito, T., Eisaki, H., and Uchida, S. (2014). Strong electronic correlations in iron pnictides: comparison of optical spectra for BaFe₂As₂-related compounds. *J. Phys. Soc. Jpn.* *83*, 104703.

Dai, P.C., Hu, J.P., and Dagotto, E. (2012). Magnetism and its microscopic origin in iron-based high-temperature superconductors. *Nat. Phys.* *8*, 709-718.

Saparov, B., and Sefat, A.S. (2012). Metallic properties of Ba₂Cu₃P₄ and BaCu₂Pn₂ (Pn=As, Sb). *J. Solid State Chem.* *191*, 213-219.

Yakita, H., Ogino, H., Okada, T., Yamamoto, A., Kishio, K., Tohei, T., Ikuhara, Y., Gotoh, Y., Fujihisa, H., Kataoka, K., Eisaki, H., and Shimoyama, J. (2014). A new layered iron arsenide superconductor: (Ca,Pr)FeAs₂. *J. Am. Chem. Soc.* *136*, 846-849.

Dünner, J., and Mewis, A. (1995). BaCu₆P₂ and BaCu₆As₂ - two compounds with a periodic intergrowth of ThCr₂Si₂ and Cu structure-type segments. *J. Alloys and Compd.* *221*, 65-69.

Huang, Q., Qiu, Y., Bao, W., Green, M.A., Lynn, J.W., Gasparovic, Y.C., Wu, T., Wu, G., and Chen, X.H.

- (2008). Neutron-diffraction measurements of magnetic order and a structural transition in the parent BaFe_2As_2 compound of FeAs-Based high-temperature superconductors. *Phys. Rev. Lett.* **101**, 257003.
- Chen, X.L., Liang, J.K., Wang, Y., Wu, F., and Rao, G.H. (1995). Superconductivity in $\text{Y}_{0.6}\text{Pr}_{0.4}\text{Ba}_{2-x}\text{Sr}_x\text{Cu}_3\text{O}_{7-\delta}$: The role of apical oxygen in hybridization. *Phys. Rev. B* **51**, 16444.
- Chen, X.L., Liang, J.K., Xie, S.S., Qiao, Z.Y., Tong, X.S., and Xing, X.R. (1992). Superconductivity and magnetic properties in $\text{Pr}_{0.2}\text{Yb}_{0.8-x}\text{La}_x\text{Ba}_2\text{Cu}_3\text{O}_{7-\delta}$. *Z. Phys.* **88**, 1-4.
- Neilson, J.R., McQueen, T.M., Llobet, A., Wen, J., and Suchoamel, M.R. (2013). Charge density wave fluctuations, heavy electrons, and superconductivity in KNi_2S_2 . *Phys. Rev. B* **87**, 045124.
- Popovich, P., Boris, A.V., Dolgov, O.V., Golubov, A.A., Sun, D.L., Lin, C.T., Kremer, R.K., and Keimer, B. (2010). Specific heat measurements of $\text{Ba}_{0.68}\text{K}_{0.32}\text{Fe}_2\text{As}_2$ single crystals: evidence for a multiband strong-coupling superconducting state. *Phys. Rev. Lett.* **105**, 027003.
- Mu, G., Wang, Y., Shan, L., and Wen, H.H. (2007). Possible nodeless superconductivity in the noncentrosymmetric superconductor $\text{Mg}_{12-\delta}\text{Ir}_{19}\text{B}_{16}$. *Phys. Rev. B* **76**, 064527.
- Uchida, S. (2015). High temperature superconductivity: the road to higher critical temperature. (Springer Verlag).
- Jia, S., Jiramongkolchai, P., Suchoamel, M.R., Toby, B.H., Checkelsky, J.G., Ong, N.P., and Cava, R.J. (2011). Ferromagnetic quantum critical point induced by dimer-breaking in $\text{SrCo}_2(\text{Ge}_{1-x}\text{P}_x)_2$. *Nat. Phys.* **7**, 207-210.
- Guo, J.G., Qi, Y.P., Matsuishi, S., and Hosono, H. (2012). T_c Maximum in solid solution of Pyrite $\text{IrSe}_2\text{-RhSe}_2$ induced by destabilization of anion dimers. *J. Am. Chem. Soc.* **134**, 20001-20004.
- Radaelli, P.G., Horibe, Y., Gutmann, M.J., Ishibashi, H., Chen, C.H., Ibberson, R.M., Koyama, Y., Hor, Y.S., Kiryukhin, V., and Cheong, S.W. (2002). Formation of isomorphous Ir^{3+} and Ir^{4+} octamers and spin dimerization in the spinel CuIr_2S_4 . *Nature* **416**, 155-158.
- Hoffmann, R., and Zheng, C. (1985). Making and breaking bonds in the solid state: The thorium chromium silicide (ThCr_2Si_2) structure. *J. Phys. Chem.* **89**, 4175-4181.
- Hoffmann, R. (1988). Solids and surfaces: a chemist's view of bonding in extended structures (VCH).
- Singh, D.J., and Du, M.H. (2008). Density functional study of $\text{LaFeAsO}_{1-x}\text{F}_x$: a Low carrier density superconductor near itinerant magnetism. *Phys. Rev. Lett.* **100**, 237003.
- Dong, J., Zhang, H.J., Xu, G., Li, Z., Li, G., Hu, W.Z., Wu, D., Chen, G.F., Dai, X., Luo, J.L., Fang, Z.,

and Wang, N.L. (2008). Competing orders and spin-density-wave instability in $\text{La}(\text{O}_{1-x}\text{F}_x)\text{FeAs}$. *Europhys. Lett.* **83**, 27006.

Subedi, A., and Singh, D.J. (2008). Density functional study of BaNi_2As_2 : Electronic structure, phonons, and electron-phonon superconductivity. *Phys. Rev. B* **78**, 132511.

Boeri, L., Dolgov, O.V., and Golubov, A.A. (2009). Electron-phonon properties of pnictide superconductors. *Physica C* **469**, 628–634.

Li, Y.K., Luo, Y.K., Li, L., Chen, B., Xu, X.F., Dai, J.H., Yang, X.J., Zhang, L., Cao, G.H., and Xu, Z.A. (2014). Kramers non-magnetic superconductivity in LnNiAsO superconductors. *J. Phys.: Condens. Matter* **26**, 425701.

Zhao, J., Huang, Q., de La Cruz, C., Li, S.L., Lynn, J.W., Chen, Y., Green, M.A., Chen, G.F., Li, G., Li, Z., Luo, J.L., Wang, N.L., and Dai, P.C. (2008). Structural and magnetic phase diagram of $\text{CeFeAsO}_{1-x}\text{F}_x$ and its relation to high-temperature superconductivity. *Nat. Mater.* **7**, 953-959.